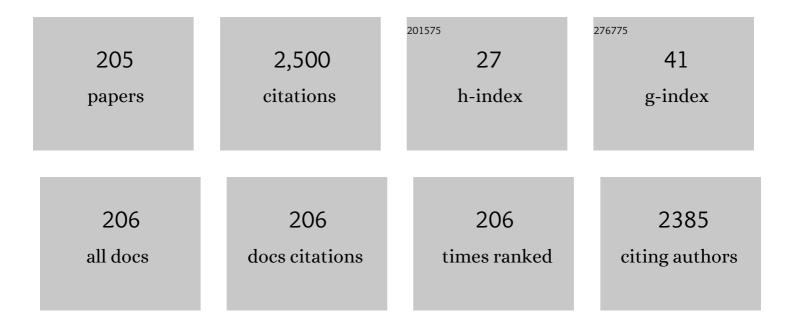
List of Publications by Year in descending order

Source: https://exaly.com/author-pdf/4023890/publications.pdf Version: 2024-02-01



#	Article	IF	CITATIONS
1	First principles study on organic cation A-site doping in CsPbI3 perovskite. Computational Materials Science, 2022, 203, 111090.	1.4	5
2	Surface functionalization of few-layer graphene on <mml:math xmlns:mml="http://www.w3.org/1998/Math/MathML" display="inline" id="d1e120" altimg="si50.svg"><mml:mi>β</mml:mi>-SiC(001) by Neutral Red dye. Applied Surface Science, 2022, 585, 152542.</mml:math 	3.1	4
3	Experimental studies of fatigue strength and surface electrical resistance of aluminum wire of overhead power transmission lines. Safety and Reliability of Power Industry, 2022, 14, 189-195.	0.1	2
4	The Structure of the Near-Surface Layer of the AAAC Overhead Power Line Wires after Operation and Its Effect on Their Elastic, Microplastic, and Electroresistance Properties. Crystals, 2022, 12, 166.	1.0	4
5	A Blueprint for the Synthesis and Characterization of Thiolated Graphene. Nanomaterials, 2022, 12, 45.	1.9	3
6	Guiding graphene derivatization for covalent immobilization of aptamers. Carbon, 2022, 196, 264-279.	5.4	7
7	Stress control in thick AlN/c-Al2O3 templates grown by plasma-assisted molecular beam epitaxy. Semiconductor Science and Technology, 2021, 36, 035007.	1.0	9
8	Molecular-Dynamics Study of Dimer Formation on a GaAs (001) Surface at Low Temperatures. Semiconductors, 2021, 55, 175-178.	0.2	0
9	Decoupling the Positive and Negative Aging Processes of Perovskite Light-Emitting Diodes Using a Thin Interlayer of Ionic Liquid. Journal of Physical Chemistry Letters, 2021, 12, 7783-7791.	2.1	8
10	Intrinsic point defects in halide double perovskite Cs2NaBiCl6 insight from first-principles. Thin Solid Films, 2021, 732, 138781.	0.8	4
11	Highâ€Quality Bulk βâ€Ga ₂ O ₃ and βâ€{Al _{<i>x</i>} Ga _{1â^²<i>x</i>}) ₂ O ₃ Crystals: Growth and Properties. Physica Status Solidi (A) Applications and Materials Science, 2021, 218, 2100335.	0.8	11
12	Modulating nitrogen species via N-doping and post annealing of graphene derivatives: XPS and XAS examination. Carbon, 2021, 182, 593-604.	5.4	66
13	Mid-IR-Sensitive n/p-Junction Fabricated on p-Type Si Surface via Ultrashort Pulse Laser n-Type Hyperdoping and High-Temperature Annealing. ACS Applied Electronic Materials, 2021, 3, 769-777.	2.0	1
14	Near-far IR photoconductivity damping in hyperdoped Si at low temperatures. Optical Materials Express, 2021, 11, 3792.	1.6	6
15	Valence Band Structure Engineering in Graphene Derivatives. Small, 2021, 17, 2104316.	5.2	8
16	Modification of the Structural, Microstructural, and Elastoplastic Properties of Aluminum Wires after Operation. Metals, 2021, 11, 1955.	1.0	9
17	Effect of stoichiometric conditions and growth mode on threading dislocations filtering in AIN/c-AI2O3 templates grown by PA MBE. Superlattices and Microstructures, 2020, 138, 106368.	1.4	19
18	Mn4+ doped zero-dimensional organic-inorganic hybrid material with narrow-red emission. Journal of Luminescence, 2020, 228, 117661.	1.5	20

#	Article	IF	CITATIONS
19	A Study of the Photoresponse in Graphene Produced by Chemical Vapor Deposition. Semiconductors, 2020, 54, 991-998.	0.2	0

20 Mechanism of Thermal Charge Relaxation in Poled Silicate Glasses in a Wide Temperature Range (From) Tj ETQq0 0.0 rgBT /Oyerlock 10

21	Laser Formation of Colloidal Sulfur- and Carbon-Doped Silicon Nanoparticles. Optics and Spectroscopy (English Translation of Optika I Spektroskopiya), 2020, 128, 897-901.	0.2	2
22	Unveiling a facile approach for large-scale synthesis of N-doped graphene with tuned electrical properties. 2D Materials, 2020, 7, 045001.	2.0	31
23	Self-trapped-induced energy funneling and broadband emission in the Mn2+ doped two-dimensional perovskite. Journal of Luminescence, 2020, 226, 117457.	1.5	7
24	Multifunctional Sulfurâ€Hyperdoped Silicon Nanoparticles with Engineered Midâ€Infrared Sulfurâ€Impurity and Freeâ€Carrier Absorption. Particle and Particle Systems Characterization, 2020, 37, 2000010.	1.2	5
25	From graphene oxide towards aminated graphene: facile synthesis, its structure and electronic properties. Scientific Reports, 2020, 10, 6902.	1.6	114
26	Establishing the applicability of the laser diffraction technique for the graphene oxide platelets lateral size measurements. Journal of Physics: Conference Series, 2020, 1695, 012070.	0.3	8
27	Size-Dependent Bioactivity of Silver Nanoparticles: Antibacterial Properties, Influence on Copper Status in Mice, and Whole-Body Turnover. Nanotechnology, Science and Applications, 2020, Volume 13, 137-157.	4.6	33
28	On the synthesis of the carboxylated graphene via graphene oxide liquid-phase modification with alkaline solutions. Journal of Physics: Conference Series, 2020, 1695, 012008.	0.3	3
29	The Influence of Reactor Pressure on the Properties of GaN Layers Grown by MOVPE. Technical Physics Letters, 2020, 46, 1211-1214.	0.2	2
30	Influence of doping profile of GaN:Fe buffer layer on the properties of AlGaN/AlN/GaN heterostructures for high-electron mobility transistors. Journal of Physics: Conference Series, 2020, 1697, 012206.	0.3	3
31	Smoothing the Surface of Gallium Antimonide. Technical Physics Letters, 2020, 46, 1203-1205.	0.2	0
32	Novel approach of controllable stoichiometric fabrication of alloyed Au/Ag nanoparticles by nanosecond laser ablation of thin bi-layered films in water. Laser Physics Letters, 2019, 16, 096002.	0.6	12
33	Crystal Structure, Raman Spectroscopy and Dielectric Properties of New Semiorganic Crystals Based on 2-Methylbenzimidazole. Crystals, 2019, 9, 573.	1.0	11
34	Insulating GaN Epilayers Co-Doped with Iron and Carbon. Technical Physics Letters, 2019, 45, 723-726.	0.2	4
35	Molecular-Dynamics Simulation of the Low-Temperature Surface Reconstruction of a GaAs(001) Surface during the Nanoindentation Process. Semiconductors, 2019, 53, 1386-1388.	0.2	2
36	The Study of Nanoindentation of Atomically Flat GaAs Surface using the Tip of Atomic-Force Microscope. Semiconductors, 2019, 53, 2110-2114.	0.2	0

#	Article	IF	CITATIONS
37	Stress evolution during growth of AlN templates on c-Al2O3 substrates by plasma-assisted molecular beam epitaxy. Journal of Physics: Conference Series, 2019, 1400, 055010.	0.3	0
38	Boson Peak Related to Ga Nanoclusters in AlGaN Layers Grown by Plasma-Assisted Molecular Beam Epitaxy at Ga-Rich Conditions. Semiconductors, 2019, 53, 1479-1488.	0.2	1
39	Characterization of optically inhomogeneous polymer layers with silver nanoparticles by spectroscopic ellipsometry. Journal of Physics: Conference Series, 2019, 1400, 055041.	0.3	1
40	Wavelength selective saturation in optical absorption of array of self-organized InAs/GaAs QDs. , 2019, , .		0
41	Metamorphic InAs(Sb)/InGaAs/InAlAs nanoheterostructures grown on GaAs for efficient mid-IR emitters. Progress in Crystal Growth and Characterization of Materials, 2019, 65, 20-35.	1.8	17
42	Relief micro- and nanostructures by the reactive ion and chemical etching of poled glasses. Optical Materials Express, 2019, 9, 3059.	1.6	9
43	Features of the Formation of Ohmic Contacts to n+-InN. Ukrainian Journal of Physics, 2019, 64, 56.	0.1	0
44	On the origin of the low-temperature band in depolarization current spectra of poled multicomponent silicate glasses. Applied Physics Letters, 2018, 112, 151603.	1.5	2
45	Barrier height modification and mechanism of carrier transport in Ni/ <i>in situ</i> grown Si ₃ N ₄ /n-GaN Schottky contacts. Semiconductor Science and Technology, 2018, 33, 025009.	1.0	6
46	Optimization of the Structural Properties and Surface Morphology of a Convex-Graded In x Al1–xAs (x) Tj ETQq	0 0 0 rgB⊺ 0.2	[/Qverlock 1
47	Milligram-per-second femtosecond laser production of Se nanoparticle inks and ink-jet printing of nanophotonic 2D-patterns. Applied Surface Science, 2018, 436, 662-669.	3.1	28
48	New method for MBE growth of GaAs nanowires on silicon using colloidal Au nanoparticles. Nanotechnology, 2018, 29, 045602.	1.3	6
49	Features of the Selective Growth of GaN Nanorods on Patterned c-Sapphire Substrates of Various Configurations. Semiconductors, 2018, 52, 1770-1774.	0.2	2
50	Dependence of leakage current in Ni/Si ₃ N ₄ /n-GaN Schottky diodes on deposition conditions of silicon nitride. Semiconductor Science and Technology, 2018, 33, 115008.	1.0	6
51	Growth of III-N/graphene heterostructures in single vapor phase epitaxial process. Journal of Crystal Growth, 2018, 504, 1-6.	0.7	14
52	Facile reduction of graphene oxide suspensions and films using glass wafers. Scientific Reports, 2018, 8, 14154.	1.6	110
53	Control of Wigner localization and electron cavity effects in near-field emission spectra of In(Ga)P/GaInP quantum-dot structures. Physical Review B, 2018, 97, .	1.1	17
54	Large-Scale Laser Fabrication of Antifouling Silicon-Surface Nanosheet Arrays via Nanoplasmonic Ablative Self-Organization in Liquid CS ₂ Tracked by a Sulfur Dopant. ACS Applied Nano Materials, 2018, 1, 2461-2468.	2.4	36

#	Article	IF	CITATIONS
55	Density Control of InP/GaInP Quantum Dots Grown by Metal-Organic Vapor-Phase Epitaxy. Semiconductors, 2018, 52, 497-501.	0.2	2
56	Metal-Semiconductor Nanoheterostructures with an AlGaN Quantum Well and In Situ Formed Surface Al Nanoislands. Semiconductors, 2018, 52, 622-624.	0.2	0
57	Elastic and Piezoelectric Parameters of the Crystals of Histidine Phosphite L-Hist · H3ĐĐž3 Measured by the Method of Electromechanical Resonance. Technical Physics Letters, 2018, 44, 118-122.	0.2	2
58	The Effect of the Method by Which a High-Resistivity GaN Buffer Layer Is Formed on Properties of InAIN/GaN and AlGaN/GaN Heterostructures with 2D Electron Gas. Technical Physics Letters, 2018, 44, 577-580.	0.2	1
59	Controllable spherical aggregation of monodisperse carbon nanodots. Nanoscale, 2018, 10, 13223-13235.	2.8	32
60	Influence of light incident angle on reflectance spectra of metals processed by color laser marking technology. Optical and Quantum Electronics, 2017, 49, 1.	1.5	8
61	InSb/InAs/InGa(Al)As/GaAs(0 0 1) metamorphic nanoheterostructures grown by MBE and emitting beyond 3 î¼m. Journal of Crystal Growth, 2017, 477, 97-99.	0.7	14
62	Spherical tokamak Globus-M2: design, integration, construction. Nuclear Fusion, 2017, 57, 066047.	1.6	83
63	Correlated topographic and structural modification on Si surface during multi-shot femtosecond laser exposures: Si nanopolymorphs as potential local structural nanomarkers. Applied Surface Science, 2017, 416, 988-995.	3.1	12
64	Electrical and optical properties of convex-type metamorphic In _{0.75} Ga _{0.25} As/In _{0.7} Al _{0.3} As quantum well structures grown by MBE on GaAs. Materials Research Express, 2017, 4, 105902.	0.8	0
65	Metal organic vapor phase epitaxy growth of (Al)GaN heterostructures on SiC/Si(111) templates synthesized by topochemical method of atoms substitution. Physica Status Solidi (A) Applications and Materials Science, 2017, 214, 1700190.	0.8	5
66	Delayed avalanche breakdown of high-voltage silicon diodes: Various structures exhibit different picosecond-range switching behavior. Journal of Applied Physics, 2017, 122, .	1.1	17
67	Stress generation and relaxation in (Al,Ga)N/6H-SiC heterostructure grown by plasma-assisted molecular-beam epitaxy. Technical Physics Letters, 2017, 43, 443-446.	0.2	3
68	Rehybridization of carbon on facets of detonation diamond nanocrystals and forming hydrosols of individual particles. Carbon, 2017, 122, 737-745.	5.4	72
69	Molecular dynamics simulations of GaAs-crystal surface modifications during nanoindentation with AFM tip Journal of Physics: Conference Series, 2017, 917, 092018.	0.3	1
70	The Extracellular Domain of Human High Affinity Copper Transporter (hNdCTR1), Synthesized by E. coli Cells, Chelates Silver and Copper Ions In Vivo. Biomolecules, 2017, 7, 78.	1.8	6
71	New silver nanoparticles induce apoptosis-like process in E. coli and interfere with mammalian copper metabolism. International Journal of Nanomedicine, 2016, Volume 11, 6561-6574.	3.3	20
72	Increasing the quantum efficiency of InAs/GaAs QD arrays for solar cells grown by MOVPE without using strainâ€balance technology. Progress in Photovoltaics: Research and Applications, 2016, 24, 1261-1271.	4.4	36

#	Article	IF	CITATIONS
73	Nanoscale Perforation of Graphene Oxide during Photoreduction Process in the Argon Atmosphere. Journal of Physical Chemistry C, 2016, 120, 28261-28269.	1.5	85
74	Increasing the quantum efficiency of GaAs solar cells by embedding InAs quantum dots. Journal of Physics: Conference Series, 2016, 769, 012036.	0.3	0
75	Ga–In intermixing, intrinsic doping, and Wigner localization in the emission spectra of self-organized InP/GaInP quantum dots. Journal Physics D: Applied Physics, 2016, 49, 475301.	1.3	17
76	Electric-field domain boundary instability in weakly coupled semiconductor superlattices. Journal of Applied Physics, 2016, 119, .	1.1	2
77	Measuring the height-to-height correlation function of corrugation in suspended graphene. Ultramicroscopy, 2016, 165, 1-7.	0.8	4
78	Experimental study of cyclic action of plasma on tungsten. Technical Physics, 2016, 61, 370-376.	0.2	6
79	Reduction of the graphene oxide films by soft UV irradiation. , 2016, , .		0
80	A study of distributed dielectric bragg reflectors for vertically emitting lasers of the near-IR range. Technical Physics Letters, 2016, 42, 1049-1053.	0.2	5
81	P-InAsSbP/n-InAs single heterostructure back-side illuminated 8×8 photodiode array. Infrared Physics and Technology, 2016, 78, 249-253.	1.3	7
82	Chloride epitaxy of β-Ga2O3 layers grown on c-sapphire substrates. Semiconductors, 2016, 50, 980-983.	0.2	5
83	The influence of growth conditions on the surface morphology and development of mechanical stresses in Al(Ga)N layers during metalorganic vapor phase epitaxy. Technical Physics Letters, 2016, 42, 431-434.	0.2	0
84	Comparative studies of CdSe/ZnSe quantum dot structures epitaxially grown with or without a sub-monolayer CdTe stressor. Physica Status Solidi C: Current Topics in Solid State Physics, 2016, 13, 514-517.	0.8	9
85	Low dark current P- InAsSbP /n- InAs/N-InAsSbP/n + - InAs double heterostructure back-side illuminated photodiodes. Infrared Physics and Technology, 2016, 76, 542-545.	1.3	7
86	Study of GaN doping with carbon from propane in a wide range of MOVPE conditions. Journal of Crystal Growth, 2016, 449, 108-113.	0.7	15
87	Picosecond-Range Avalanche Switching of High-Voltage Diodes: Si Versus GaAs Structures. IEEE Transactions on Plasma Science, 2016, 44, 1941-1946.	0.6	18
88	Semi-insulating GaN:C epilayers grown by metalorganic vapor phase epitaxy using propane as a carbon source. Technical Physics Letters, 2016, 42, 539-542.	0.2	5
89	InAsSbP/InAs 0.9 Sb 0.1 /InAs DH photodiodes (λ 0.1 = 5.2 μm, 300 K) operating in the 77–353 Đš temperati range. Infrared Physics and Technology, 2015, 73, 232-237.	ure 1.3	10
90	Estimation of the effective electron-capture cross section in the emission processes from arrays of vertically coupled InAs quantum dots in the n-GaAs matrix. Journal of Physics: Conference Series, 2015, 643, 012081.	0.3	0

#	Article	IF	CITATIONS
91	Carrier trapping study on a Ge nanocrystal by two-pass lift mode electrostatic force microscopy. Materials Research Express, 2015, 2, 035001.	0.8	1
92	Effect of the interaction conditions of the probe of an atomic-force microscope with the n-GaAs surface on the triboelectrization phenomenon. Semiconductors, 2015, 49, 1057-1061.	0.2	2
93	Cylindrical multilayer metal–dielectric structures. Technical Physics Letters, 2015, 41, 1097-1098.	0.2	3
94	Gallium nitride nanowires and microwires with exceptional length grown by metal organic chemical vapor deposition via titanium film. Journal of Applied Physics, 2015, 117, 024301.	1.1	8
95	Formation of silver fractal structures in ion-exchange glasses under poling. Technical Physics, 2015, 60, 270-274.	0.2	4
96	Pulsed growth techniques in plasma-assisted molecular beam epitaxy of Al Ga1â^'N layers with medium Al content (x=0.4–0.6). Journal of Crystal Growth, 2015, 425, 9-12.	0.7	14
97	Temperature dependences of the contact resistivity in ohmic contacts to n +-InN. Semiconductors, 2015, 49, 461-471.	0.2	6
98	Plasmon-induced enhancement of yellow-red luminescence in InGaN/Au nanocomposites. Semiconductors, 2015, 49, 247-253.	0.2	7
99	Defect engineering in AlGaN-based UV optoelectronic heterostructures grown on c-Al2O3 by plasma-assisted molecular beam epitaxy. Materials Research Society Symposia Proceedings, 2015, 1741, 47.	0.1	1
100	Determination of the technological growth parameters in the InAs-GaAs system for the MOCVD synthesis of "Multimodal―InAs QDs. Semiconductors, 2015, 49, 1111-1118.	0.2	10
101	High-voltage subnanosecond avalanche sharpening diodes: A comparative study of silicon and gallium arsenide structures. , 2015, , .		0
102	Experimental Demonstration of Reduced Light Absorption by Intracavity Metallic Layers in Tamm Plasmon-based Microcavity. Plasmonics, 2015, 10, 281-284.	1.8	28
103	P-InAsSbP/n 0-InAs/n +-InAs photodiodes for operation at moderate cooling (150–220 K). Semiconductors, 2014, 48, 1359-1362.	0.2	7
104	Multiperiod quantum-cascade nanoheterostructures: Epitaxy and diagnostics. Semiconductors, 2014, 48, 1600-1604.	0.2	9
105	Dependence of the efficiency of III-N blue LEDs on the structural perfection of GaN epitaxial buffer layers. Semiconductors, 2014, 48, 53-57.	0.2	9
106	Molecular beam epitaxy of AlGaAs/Zn(Mn)Se hybrid nanostructures with InAs/AlGaAs quantum dots near the heterovalent interface. Semiconductors, 2014, 48, 34-41.	0.2	0
107	Analysis of thermal emission processes of electrons from arrays of InAs quantum dots in the space charge region of GaAs matrix. Semiconductors, 2014, 48, 1155-1160.	0.2	2
108	Study of the electrical properties of individual (Ga,Mn)As nanowires. Semiconductors, 2014, 48, 344-349.	0.2	2

#	Article	IF	CITATIONS
109	Optimization of carrier mobility in luminescence layers based on europium β-diketonates in hybrid light-emitting structures. Semiconductors, 2014, 48, 369-372.	0.2	10
110	Cooled P-InAsSbP/n-InAs/N-InAsSbP double heterostructure photodiodes. Infrared Physics and Technology, 2014, 64, 62-65.	1.3	6
111	Organic light-emitting diodes based on polyvinylcarbazole films doped with polymer nanoparticles. Physics of the Solid State, 2013, 55, 675-680.	0.2	19
112	Formation of silver nanoparticles on the silicate glass surface after ion exchange. Physics of the Solid State, 2013, 55, 1272-1278.	0.2	39
113	Mechanism of electronic-excitation transfer in organic light-emitting devices based on semiconductor quantum dots. Semiconductors, 2013, 47, 971-977.	0.2	16
114	Statistical analysis of AFM topographic images of self-assembled quantum dots. Semiconductors, 2013, 47, 930-934.	0.2	9
115	Integrated characterization of multilayer periodic systems with nanosized layers as applied to Mo/Si structures. Physics of the Solid State, 2013, 55, 648-658.	0.2	2
116	Ultra-low density InAs quantum dots. Semiconductors, 2013, 47, 1324-1327.	0.2	1
117	Control of threading dislocation density at the initial growth stage of AlN on c-sapphire in plasma-assisted MBE. Journal of Crystal Growth, 2013, 378, 319-322.	0.7	54
118	Local triboelectrification of an n-GaAs surface using the tip of an atomic-force microscope. Semiconductors, 2013, 47, 1170-1173.	0.2	6
119	Single-layer graphene oxide films on a silicon surface. Technical Physics, 2013, 58, 1614-1618.	0.2	20
120	Selective area growth of GaN on râ€plane sapphire by MOCVD. Physica Status Solidi C: Current Topics in Solid State Physics, 2013, 10, 373-376.	0.8	1
121	Sputter depth profiling of Mo/B4C/Si and Mo/Si multilayer nanostructures: A round-robin characterization by different techniques. Thin Solid Films, 2013, 540, 96-105.	0.8	24
122	Influence of the carrier Gas, trimethylgallium flow, and growth time on the character of the selective epitaxy of GaN. Semiconductors, 2013, 47, 437-442.	0.2	2
123	Various types of GaN/InGaN nanostructures grown by MOCVD on Si(111) substrate. Physica Status Solidi C: Current Topics in Solid State Physics, 2013, 10, 441-444.	0.8	3
124	Characterization of defects in colloidal CdSe nanocrystals by the modified thermostimulated luminescence technique. Semiconductors, 2013, 47, 1328-1332.	0.2	19
125	Investigation of the morphological features of silver nanoparticles in the near-surface layers of glass when they are synthesized by heat treatment in water vapor. Journal of Optical Technology (A) Tj ETQq1 1	0.784314	⊦rg₿T /Overic
126	High growth rate MOVPE of Al(Ga)N in planetary reactor. Journal of Crystal Growth, 2012, 352, 209-213.	0.7	21

#	Article	IF	CITATIONS
127	Composite InGaN/GaN/InAIN heterostructures emitting in the yellow-red spectral region. Semiconductors, 2012, 46, 1281-1285.	0.2	4
128	Self-assembled silver nanoislands formed on glass surface via out-diffusion for multiple usages in SERS applications. Nanoscale Research Letters, 2012, 7, 676.	3.1	40
129	A weakly coupled semiconductor superlattice as a potential for a radio frequency modulated terahertz light emitter. Applied Physics Letters, 2012, 100, .	1.5	5
130	Electron states at electrolyte/n-GaN and electrolyte/n-InGaN interfaces. Semiconductors, 2012, 46, 755-758.	0.2	0
131	Surface electrostatic potential of inn epitaxial layers and its changes during anodic oxidization. Journal of Surface Investigation, 2012, 6, 420-423.	0.1	1
132	Double-cross epitaxial overgrowth of nonpolar gallium nitride layers. Technical Physics Letters, 2012, 38, 265-267.	0.2	1
133	Studying the formation of self-assembled (In,Mn)As quantum dots. Technical Physics Letters, 2012, 38, 460-462.	0.2	3
134	Monolayer graphene from graphite oxide. Diamond and Related Materials, 2011, 20, 105-108.	1.8	66
135	Optoelectronic structures with InAlN layers grown by MOVPE. AIP Conference Proceedings, 2011, , .	0.3	0
136	Electrochemical capacitance-voltage profiling of the free-carrier concentration in HEMT heterostructures based on InGaAs/AlGaAs/GaAs compounds. Semiconductors, 2011, 45, 811-817.	0.2	12
137	Mutual synchronization of two coupled self-oscillators based on GaAs/AlGaAs superlattices. Technical Physics, 2011, 56, 826-830.	0.2	2
138	Study of roughness in multilayer Mo–Si mirrors. Physica Status Solidi (A) Applications and Materials Science, 2011, 208, 2623-2628.	0.8	9
139	Single quantum well deep-green LEDs with buried InGaN/GaN short-period superlattice. Journal of Crystal Growth, 2011, 315, 267-271.	0.7	32
140	Influence of ex-situ AFM treatment on epitaxial growth of self-organized InAs quantum dots. Proceedings of SPIE, 2010, , .	0.8	0
141	Study of defects in heterostructures with GaPAsN and GaPN quantum wells in the GaP matrix. Semiconductors, 2010, 44, 893-897.	0.2	8
142	Capacitance-voltage characteristics of the electrolyte-n-InN surface and electron states at the interface. Semiconductors, 2010, 44, 1020-1024.	0.2	1
143	Formation of composite InGaN/GaN/InAlN quantum dots. Semiconductors, 2010, 44, 1338-1341.	0.2	3
144	High growth rate of AlN in a planetary MOVPE reactor. Technical Physics Letters, 2010, 36, 1133-1135.	0.2	4

#	Article	IF	CITATIONS
145	EFM Study on Ge Island: Carrier Charge and Storage Effect. Materials Research Society Symposia Proceedings, 2010, 1260, 1.	0.1	0
146	Electrical study of trapped charges in nanoscale Ge islands by Kelvin probe force microscopy for nonvolatile memory applications. Applied Physics Letters, 2010, 97, 263112.	1.5	13
147	Submicron Surface Relief Formation Using Thermal Poling of Glasses. E-Journal of Surface Science and Nanotechnology, 2009, 7, 617-620.	0.1	12
148	Self-oscillations in weakly coupled GaAs/AlGaAs superlattices at 77.3 K. Journal of Applied Physics, 2009, 105, 033711.	1.1	8
149	Study of the formation of InGaN quantum dots on GaN surface. Bulletin of the Russian Academy of Sciences: Physics, 2009, 73, 36-38.	0.1	1
150	Indium-rich island structures formed by in-situ nanomasking technology. Technical Physics Letters, 2009, 35, 1016-1019.	0.2	0
151	Phase separation and nonradiative carrier recombination in active regions of light-emitting devices based on InGaN quantum dots in a GaN or AlGaN matrix. Semiconductors, 2009, 43, 807-811.	0.2	1
152	Effect of carrier gas and doping profile on the surface morphology of MOVPE grown heavily doped GaN:Mg layers. Semiconductors, 2009, 43, 963-967.	0.2	22
153	The short-wavelength edge of intrinsic photoluminescence in diluted GaN x As1 â^' x alloys. Semiconductors, 2009, 43, 1267-1270.	0.2	0
154	Submicron-resolved relief formation in poled glasses and glass-metal nanocomposites. Technical Physics Letters, 2008, 34, 1030-1033.	0.2	45
155	Electron emission from multilayer ensembles of vertically coupled InAs quantum dots in an n-GaAs matrix. Semiconductors, 2008, 42, 1104-1107.	0.2	6
156	Surface states on the n-InN-electrolyte interface. Semiconductors, 2008, 42, 1416-1419.	0.2	1
157	Band bending of n-InN epilayers and exact solution of the classical Thomas–Fermi equation. Physica Status Solidi - Rapid Research Letters, 2007, 1, 159-161.	1.2	7
158	Cathodoluminescence from dilute GaN x As1â^'x solutions (x ≤0.03). Semiconductors, 2007, 41, 1297-1299.	0.2	0
159	Capacitance studies of multilayer ensembles of InAs QDs in a GaAs matrix. Semiconductors, 2007, 41, 1335-1338.	0.2	1
160	Direct observation of isolated ultrananodimensional diamond clusters using atomic force microscopy. Technical Physics Letters, 2006, 32, 561-563.	0.2	11
161	P-i-n structures based on high-ohmic gettered gallium arsenide for α particle detectors. Technical Physics Letters, 2006, 32, 987-989.	0.2	2
162	An X-ray diffraction and electron-microscopic study of the influence of gamma radiation on multilayer AlGaAs/InGaAs/GaAs heterostructures. Semiconductors, 2006, 40, 687-690.	0.2	3

#	Article	IF	CITATIONS
163	Diffusion-barrier contacts based on the TiN and Ti(Zr)Bx interstitial phases in the microwave diodes for the range of 75–350 GHz. Semiconductors, 2006, 40, 734-738.	0.2	4
164	Higher harmonics in the current oscillations in weakly coupled GaAs/AlGaAs superlattices. Semiconductors, 2006, 40, 825-828.	0.2	2
165	Optical study of resonant states in GaN x As1â^'x. Semiconductors, 2006, 40, 1162-1164.	0.2	0
166	Domain boundary instability in weakly coupled GaAs/AlGaAs superlattices. Superlattices and Microstructures, 2005, 37, 139-150.	1.4	6
167	A Study of Recombination Centers Related to As–Sb Nanoclusters in Low-Temperature Grown Gallium Arsenide. Semiconductors, 2005, 39, 33.	0.2	0
168	Electron Traps in Thin Layers of Low-Temperature-Grown Gallium Arsenide with As–Sb Nanoclusters. Semiconductors, 2005, 39, 1013.	0.2	1
169	Optical spin polarization in double charged InAs self-assembled quantum dots. Physica Status Solidi (A) Applications and Materials Science, 2005, 202, 387-391.	0.8	0
170	Capacitance spectroscopy study of InAs quantum dots and dislocations in p-GaAs matrix. AIP Conference Proceedings, 2005, , .	0.3	0
171	Breakup of the conduction band structure of diluteGaAs1â^'yNyalloys. Physical Review B, 2005, 71, .	1.1	40
172	Optical spin polarization and exchange interaction in doubly charged InAs self-assembled quantum dots. Physical Review B, 2005, 72, .	1.1	28
173	Self-sustained oscillations in weakly coupled GaAs/AlGaAs superlattices. Semiconductor Science and Technology, 2004, 19, S77-S79.	1.0	5
174	Wavelength selective charge accumulation in self-organized InAs/GaAs quantum dots. Semiconductor Science and Technology, 2004, 19, S51-S53.	1.0	3
175	Capacitance study of electron traps in low-temperature-grown GaAs. Semiconductors, 2004, 38, 387-392.	0.2	1
176	Carrier density profile in weakly coupled GaAs/AlGaAs superlattices. Semiconductors, 2004, 38, 451-454.	0.2	3
177	Spectral hole burning in self-organized quantum dots. Physica E: Low-Dimensional Systems and Nanostructures, 2004, 21, 215-218.	1.3	3
178	Optical spin polarization of holes in negatively charged InAs/GaAs self-assembled quantum dots. Physica E: Low-Dimensional Systems and Nanostructures, 2004, 21, 1018-1021.	1.3	3
179	Study of trap centres in silicon nanocrystal memories. Materials Science and Engineering B: Solid-State Materials for Advanced Technology, 2003, 102, 99-107.	1.7	6
180	Optical spin polarization in negatively charged InAs self-assembled quantum dots under applied electric field. Physica Status Solidi (B): Basic Research, 2003, 238, 250-253.	0.7	10

#	Article	IF	CITATIONS
181	Modification of GaAs by medium-energy N 2 + ions. Technical Physics, 2003, 48, 885-888.	0.2	3
182	Strain relaxation in stacked InAs/GaAs quantum dots studied by Raman scattering. Applied Physics Letters, 2003, 83, 3069-3071.	1.5	36
183	Magnetic-field-induced recovery of resonant tunneling into a disordered quantum well subband. Physical Review B, 2003, 68, .	1.1	11
184	<title>Escape of carriers photoexcited in self-organized InAs/GaAs quantum dots</title> . , 2002, , .		0
185	Photocurrent and capacitance spectroscopy of Schottky barrier structures incorporating InAs/GaAs quantum dots. Physical Review B, 2002, 65, .	1.1	35
186	Capacitance Spectroscopy of n-i-n and p-i-p GaAs Sandwich Structures with Nanoscale As Clusters in the i-Layers. Materials Research Society Symposia Proceedings, 2001, 699, 461.	0.1	0
187	Time-Resolved Capacitance Spectroscopy of Hole and Electron Levels in InAs/GaAs Quantum Dots. Physica Status Solidi (B): Basic Research, 2001, 224, 57-60.	0.7	2
188	Probing the electronic properties of disordered two-dimensional systems by means of resonant tunnelling. Nanotechnology, 2001, 12, 491-495.	1.3	3
189	Accumulation of majority charge carriers in GaAs layers containing arsenic nanoclusters. Semiconductors, 2000, 34, 1068-1072.	0.2	4
190	Modulation of the luminescence spectra of InAs self-assembled quantum dots by resonant tunneling through a quantum well. Physical Review B, 2000, 62, 13595-13598.	1.1	18
191	Hole and electron emission from InAs quantum dots. Applied Physics Letters, 2000, 76, 1573-1575.	1.5	110
192	Emission of electrons from the ground and first excited states of self-organized InAs/GaAs quantum dot structures. Journal of Electronic Materials, 1999, 28, 486-490.	1.0	33
193	Electron and hole levels of InAs quantum dots in a GaAs matrix. Superlattices and Microstructures, 1999, 25, 105-111.	1.4	6
194	Accumulation of electrons in GaAs layers grown at low temperatures and containing arsenic clusters. Semiconductors, 1998, 32, 1044-1047.	0.2	2
195	Capacitance-voltage profiling of Au/n-GaAs Schottky barrier structures containing a layer of self-organized InAs quantum dots. Semiconductors, 1998, 32, 1096-1100.	0.2	25
196	Optical studies of modulation doped InAs/GaAs quantum dots. Microelectronic Engineering, 1998, 43-44, 71-77.	1.1	2
197	Electron escape from self-assembled InAs/GaAs quantum dot stacks. Physica B: Condensed Matter, 1998, 249-251, 267-270.	1.3	8
198	Electronic structure of self-assembled InAs quantum dots in GaAs matrix. Applied Physics Letters, 1998, 73, 1092-1094.	1.5	86

#	Article	IF	CITATIONS
199	Bistability of charge accumulated in low-temperature-grown GaAs. Applied Physics Letters, 1998, 73, 2796-2798.	1.5	8
200	Simulation of the capacitance–voltage characteristics of a singleâ€quantumâ€well structure based on the selfâ€consistent solution of the Schrödinger and Poisson equations. Journal of Applied Physics, 1996, 80, 864-871.	1.1	47
201	Determination of donor and acceptor level energies by admittance spectroscopy in 6H SiC. Materials Science and Engineering B: Solid-State Materials for Advanced Technology, 1995, 29, 122-125.	1.7	14
202	Admittance spectroscopy of InAlAs/InGaAs singleâ€quantumâ€well structure with high concentration of electron traps in InAlAs layers. Journal of Applied Physics, 1995, 77, 240-243.	1.1	12
203	Generation of the EL2 defect in n-GaAs irradiated by high energy protons. Semiconductor Science and Technology, 1992, 7, 1237-1240.	1.0	22
204	Majority carrier accumulation in low-temperature-grown GaAs layer inserted into n-and p-type matrices. , 0, , .		0
205	Guiding Graphene Derivatization for the Onâ€Chip Multisensor Arrays: From the Synthesis to the Theoretical Background. Advanced Materials Technologies, 0, , 2101250.	3.0	8